ORNL
MASTER COPY

OAK RIDGE NATIONAL LABORATORY
operated by
UNION CARBIDE CORPORATION
for the
U.S. ATOMIC ENERGY COMMISSION

OAK RIDGE NATIONAL LABORATORY LIBRARIES
3 4456 0599478 3

ORNL-TM-1084
COPY NO. - 73
DATE - September 3, 1965

HFIR TARGET DESIGN STUDY

T. G. Chapman

ABSTRACT

The HFIR target design was investigated to determine the interaction of ^{242}Pu loading, number of 3/8-in.-diam target rods, neutron flux, and batch irradiation time on the production of ^{252}Cf. The study indicates that irradiation time and heat flux are the most important variables in determining the ^{252}Cf production.

The interface between the pellet and tube was studied to determine the effect of resistance to heat transfer on the maximum rod temperature. A temperature of 900°F was selected as an upper limit for normal reactor power. A metallurgical bond or heat transfer equivalent between the pellet and tube would permit a maximum heat flux of 1.5×10^6 Btu hr^{-1} ft^{-2}. A radial clearance of 0.8 mils or less would permit a maximum heat flux of 1×10^6 Btu hr^{-1} ft^{-2}.

The maximum permissible loading based on this analysis of the present design and the target material presently on hand is 310 g of $^{242}PuO_2$ (274 g of ^{242}Pu) in 31 rods. It is recommended that this loading, which is about an optimum loading for 18 to 24 months of irradiation at a heat flux of 1×10^6 Btu hr^{-1} ft^{-2}, be used.

The plutonium feed material available for the first target loading contains about 1% ^{239}Pu and 1% ^{241}Pu. The inclusion of these fissionable materials in the target results in a heat flux at the beginning of target irradiation that is slightly more than that associated with the peak ^{245}Cm concentration later in the cycle. However, the maximum rod temperature is less than 900°F.

~~NOTICE This document contains information of a preliminary nature and was prepared primarily for internal use at the Oak Ridge National Laboratory. It is subject to revision or correction and therefore does not represent a final report.~~

OK for public release.
David R. Hamrin
5/1/2009

LEGAL NOTICE

This report was prepared as an account of Government sponsored work. Neither the United States, nor the Commission, nor any person acting on behalf of the Commission:

A. Makes any warranty or representation, expressed or implied, with respect to the accuracy, completeness, or usefulness of the information contained in this report, or that the use of any information, apparatus, method, or process disclosed in this report may not infringe privately owned rights; or

B. Assumes any liabilities with respect to the use of, or for damages resulting from the use of any information, apparatus, method, or process disclosed in this report.

As used in the above, "person acting on behalf of the Commission" includes any employee or contractor of the Commission, or employee of such contractor, to the extent that such employee or contractor of the Commission, or employee of such contractor prepares, disseminates, or provides access to, any information pursuant to his employment or contract with the Commission, or his employment with such contractor.

INTRODUCTION

The plutonium loading previously specified[1] for the island target in the HFIR was ~300 g ^{242}Pu plus ~3 g ^{241}Pu, the latter isotope concentration being limited to one percent so that the initial heat generation rate would not exceed that associated with the subsequent buildup of ^{245}Cm (ref. 2). At the time these calculations were made, the weight ratio of aluminum to plutonium was estimated to be 5, and the irradiation time was assumed to be one year. The 300 g loading represented an optimum loading, in terms of maximum ^{252}Cf production, for these conditions. Since that time structural changes plus the inclusion of ^{239}Pu in the feed material on hand necessitated a revaluation of the target loading and aluminum to plutonium weight ratio.

The target consists of PuO_2-Al cylindrical pellets encased in 3/8-in.-OD by 20-in.-active-length aluminum tubes (shown by Fig. 3), which are bundled together to make up an assembly. An important heat transfer parameter associated with this type of design is the thermal resistance of the bond (or lack of bond) between the pellets and the tube. A variation in this resistance has a significant effect on the permissible heat flux and thus the metal-to-water ratio and/or weight of plutonium in the target.

METHOD OF ANALYSIS

A parametric study, based on a conceptual target design, was made on the production of ^{252}Cf in the HFIR target region. The concentration of ^{242}Pu and Al was varied in the target region with the following constant parameters: (1) 5-in. island diameter, (2) 3/8-in. individual target rod diameter, and (3) 100 Mw reactor power level. The variations in ^{242}Pu loading and number of rods, as given in Table 1, were used to determine the average neutron flux in the target region with Modric.[3] These average neutron fluxes were used in conjunction with the results of the minimum production scheme of Claiborne[2] to give the ^{252}Cf production for batch irradiation times of 4, 10, 12, 18, and 24 months. However, a maximum production scheme and contributions from nonthermal capture were

Table 1. ^{242}Pu-Al Parameter Variations

Case	^{242}Pu Loading g	No. of 3/8" Dia Rods	^{242}Pu/Rod g/Rod
1	150	15	10.0
2	150	18	8.33
3	150	21	7.14
4	150	24	6.25
5	150	27	5.55
6	175	18	9.72
7	175	21	8.33
8	175	24	7.29
9	175	27	6.48
10	175	30	5.83
11	200	21	9.52
12	200	24	8.33
13	200	27	7.41
14	200	30	6.67
15	225	24	9.33
16	225	27	8.33
17	225	30	7.50
18	225	21	10.7
19	250	24	10.4
20	250	27	9.26
21	250	30	8.33

included in the isotopic concentrations for maximizing the average heat generation to evaluate the heat removal problem. This average heat generation included the fission heat from the fissionable ^{242}Pu-^{252}Cf chain members and the deposition of gamma rays from the fuel element.

The average heat flux found from the above mentioned heat sources was converted to a hot spot value. A radial maximum-to-average power ratio was determined from the radial neutron flux distribution, whereas a constant value of 1.29 was used for the axial maximum-to-average value as found in reference 1. A local uncertainty factor of 1.25 was also applied with the flux peaking values to give a maximum heat flux. The product of the average heat flux and the three peaking values defines the heat removal problem for a design analysis.

The effects of the three variables on the ^{252}Cf production are shown in Fig. 1 for batch irradiations. Figure 2 gives the maximum heat flux versus ^{242}Pu loading for a specific number of rods. As can be seen from Fig. 1, the surfaces for about 10 to 15 months of irradiation time display almost no preference for loading, but gains in ^{252}Cf production are made with increased heat flux (lower metal-to-water ratio).

Since heat flux and maximum rod temperature are so intimately related, the final design must consider the temperature problem also. An investigation of the rod temperature pattern was conducted with the following assumptions:

1. Minimum local heat transfer coefficient was applied as recommended by Gambill.[4]
2. Al_2O_3 formation was given by the equation of Griess.[5]
3. The oxide formation was for 6 months' operation at 3/4 of the hot spot heat flux.
4. The minimum bulk water velocity was 40 ft/sec.
5. The bulk water temperature at the hot spot location was 130°F.
6. The thermal conductivity of the Al was 125 Btu hr^{-1} ft^{-1} $(°F)^{-1}$.
7. The thermal conductivity of the PuO_2-Al powder compact was 50 Btu hr^{-1} ft^{-1} $(°F)^{-1}$.
8. No axial heat conduction.
9. Eighty-five percent of the heat was generated in the pellets and 15% in the containment tube.

With these assumptions, three cases were studied for the present fabrication technique of separate pellets contained in a tube as shown in Fig. 3. The cases were:

1. Metallurgical bond or heat transfer equivalent.
2. A clearance containing gas.
3. A heat transfer resistance with no clearance.

All three cases had the same temperature distribution for the containment tube and also all cases had the same temperature profile for the pellets. The only difference in the three cases was the temperature drop at the interface. An analysis of the temperature pattern was performed for Case 1 for different heat fluxes, and the maximum temperature results are shown in Fig. 4 for a bond between pellet and containment tube. The other two cases increased the maximum temperature by the temperature drop at the interface as given in the following discussion.

For Case 2, two equations were written for a uniform clearance between the pellet and tube. The first equation relates the difference in expansion of the pellet and tube with the initial tolerance. The clearance at power will be the difference in expansion of the pellet, the expansion of the tube, and the initial clearance as given below:

$$t = C - (T_1 - T_2)\,\alpha\,R \qquad (1)$$

where

t = clearance at temperature, mils;
T_2 = average temperature of tube, °F;
T_1 = average temperature of pellets, °F;
α = linear coefficient of expansion, 13×10^{-6} in. in.$^{-1}$ (°F)$^{-1}$;
R = radius of pellet, 125 mils;
C = initial clearance, mils.

The second equation is a rearrangement of the conduction equation with constants to convert to the dimensions as used in the above equation. The second equation is

$$t = \frac{(1.2)(10^{-2})(k_g)(\Delta T_g)}{1.5F} \qquad (2)$$

where

t = clearance at temperature, mils;

k_g = gas thermal conductivity, Btu hr^{-1} ft^{-1} $(°F)^{-1}$;

ΔT_g = temperature drop across clearance at temperature, °F;

F = fractional part of a 10^6 Btu hr^{-1} ft^{-2} heat flux at outside surface of containment tube.

The average temperatures were expressed as functions of F and ΔT_g, and the two equations were solved simultaneously for

$$\Delta T_g = \frac{615C - 108F}{1 + \frac{4.92\ k_g}{F}} \quad . \tag{3}$$

A conservative estimate of ΔT_g was obtained by assuming $(4.92\ k_g)/F$ was negligible in comparison to 1. This was reasonable for the heat fluxes studied because the clearance was assumed, for design purposes, to contain mostly fission gases. Thus, an error of about 10% was made in reducing Eq. (3) to

$$\Delta T_g = 615C - 108F \quad . \tag{4}$$

Equation (4) resulted in a ΔT_g of 300 to 400°F with an initial clearance of 3/4 mil for the range of heat fluxes considered. The initial clearance will almost disappear with thermal expansion. In fact, the clearance at temperature will be less than the combined initial surface roughnesses of 125 μin. Thus, the pellet will probably have metal-to-metal contact and will be considered as Case 3. A temperature of 400°F was added to Case 1 to obtain Case 2 as shown in Fig. 4 as the curve for a 3/4-mil initial clearance.

In Case 3, the assumption is made that the pellet and containment tube have intermittent areas of metal-to-metal contact. Parallel heat flow paths will be established with both gas and metal conductance contributing to the heat removal process. An idealized model[6] for predicting the thermal conductance between metallic surfaces has been proposed and is in good agreement with the experiment data. The analysis depends on surface roughness, apparent contact pressure, gas and metal conductivities,

number of contact points, and area of contact. The reference predicts the thermal conductance versus apparent pressure for Al–U surfaces at a mean contact temperature of 750°F, a 150-rms combined surface roughness, with assumed profiles obtained from Al and iron samples and a 50% He + 50% (Xe + Kr) by volume gas mixture. The use of the above predicted conductance should be conservative since the lower Al pellet yield stress[7] would provide more contact area than the U for the temperature range of interest. An approximation to the thermal conductance is

$$h = 1000\ (P_A)^{1/2} \tag{5}$$

where

h = contact thermal conductance Btu hr^{-1} ft^{-2} $(°F)^{-1}$

P_A = apparent pressure, psi

An additional equation is the expansion of the tube and pellet which is written as

$$(T_1 - T_2)\ \alpha\ R = C + \frac{P_A\ R^2}{E\ b} \tag{6}$$

where

T_2 = average temperature of tube, °F

T_1 = average temperature of pellet, °F

α = linear coefficient of expansion, 13×10^{-6} in. $in.^{-1}$ $(°F)^{-1}$

R = radius of pellet, 0.125 in.

C = initial fabrication clearance, in.

E = modulus of elasticity of tube, 10×10^6 lbs $in.^{-2}$

b = thickness of tube, 0.125 in.

The heat flux at the contact surface can be written as

$$(1.5)(.85)(F)(10^{-6}) = h\ \Delta T_c \tag{7}$$

where

F = fractional part of 10^6 Btu hr^{-1} ft^{-2} heat flux

h = contact thermal conductance Btu hr^{-1} ft^{-2} $(°F)^{-1}$

ΔT_c = temperature drop at contact surface, °F

and when combined with Eqs. (5) and (6) yields

$$\Delta T_c = 615C - 108F + 615 \left(\frac{2 \times 10^{-5} F}{\Delta T_c}\right)^2 \qquad (8)$$

The last term in Eq. (8) is negligible in comparison with the other terms for this study. Therefore, the equation for the temperature drop at the contact surface is

$$\Delta T_c = 615C - 108F \qquad (9)$$

which is the same as Eq. (4). Therefore, Case 2 and Case 3 produce about the same temperature drop at the pellet and tube interface and the temperature is shown in Fig. 4 for a 3/4-mil initial clearance.

RESULTS AND CONCLUSIONS

With rod temperatures calculated for the heat flux range of interest, the selection of a maximum temperature for design purposes will be discussed. The maximum rod temperature was fixed at 1220°F. (This corresponds to the melting point of aluminum in order to eliminate any possibility of settling of the PuO_2 particles.) This gives a 1090°F maximum temperature difference between the maximum rod temperature and bulk water temperature. This value was reduced by 30% to be consistent with the design of the reactor control system, since the power level scram point is set 30% greater than the 100 Mw design power level. In addition, a 10% reduction is taken for contingencies. The application of the above factors gives 900°F as the maximum rod temperature. Applying the 900°F temperature criterion to Fig. 4 establishes the heat flux at 1×10^6 Btu hr^{-1} ft^{-2} for the target design shown in Fig. 3. Limiting the heat flux to 1×10^6 Btu hr^{-1} ft^{-2} in Fig. 1 gives an optimum ^{242}Pu loading of 190 g for one years' irradiation time. The corresponding number of rods as determined from Fig. 2 is 26.

The aforementioned optimization was determined to meet one HFIR design objective which was to maximize the ^{252}Cf production in one year of target irradiation. It is evident from Fig. 1 that this design objective is not seriously compromised with large variations in ^{242}Pu loading (e.g., a 50% change in ^{242}Pu loading produces a 10% variation in

^{252}Cf production). Therefore, other objectives could be considered in determining the ^{242}Pu loading. Such considerations could be the amount of material to process, establishment of a recycle schedule, or longer irradiation periods. Thus, the question arises: What is the maximum loading for the target design shown in Fig. 3?

The target assembly has 31 matrix positions with two proposals for utilizing these positions. One proposal has all 31 positions occupied with target rods, whereas an alternate proposal has 30 target rods with a centrally located rabbit facility. The solution to the above question corresponding to each proposal can be determined from Fig. 2 for a heat flux of 1×10^6 Btu hr^{-1} ft^{-2}. The maximum loadings are 283 g of ^{242}Pu (318 g of $^{242}PuO_2$) in 31 rods and 265 g of ^{242}Pu (300 g of $^{242}PuO_2$) in 30 rods.

An examination of Fig. 1 for about 275 g of ^{242}Pu and a heat flux of 1×10^6 Btu hr^{-1} ft^{-2} indicates about optimum ^{252}Cf production for irradiation times of 18 to 24 months. Therefore, it is recommended that each target rod contain 10 g of $^{242}PuO_2$ (8.83 g of ^{242}Pu) so that either 30 or 31 target rods can be inserted in the target region without exceeding the heat flux criterion or appreciably decreasing the ^{252}Cf production.

An investigation was conducted on the effect on ^{252}Cf production of the initial clearance between the pellet and the containment tube. The maximum temperature was held constant at 900°F by adjusting the ^{242}Pu loading as the clearance was varied. The study indicated that 8.83 g ^{242}Pu (10 g $^{242}PuO_2$) per rod would be permissible for initial clearances up to 0.8 mil between the pellet and containment tube. Larger clearances required lower ^{242}Pu loadings; consequently, the production of ^{252}Cf would be reduced. The ^{252}Cf production as a function of the aforementioned clearance is shown in Fig. 5. The figure illustrates the need to guarantee that the target rods have an initial radial gap no greater than 0.8 mil between the pellet and the containment tube. Destructive tests indicate a maximum initial clearance of 0.5 mil.

Another problem analyzed was the permissible reactor power level for a target rod that contains ^{239}Pu and ^{241}Pu as the heat source. While these isotopes will disappear exponentially with time due to neutron absorption, the heat generation at any time will be proportional to the

number of fissionable atoms present. Thus the heat generation can be related to the initial value as

$$H_i(t) = \sum_i H_i(o) \exp\left[-(\sigma_i^c + \sigma_i^f)\, \phi\, t\right] \tag{11}$$

where

$H(t)$ = heat generation at time t, Btu hr^{-1} ft^{-3};
$H(o)$ = initial heat generation for the $i^{\underline{th}}$ isotope, Btu hr^{-1} ft^{-3};
σ_i^c = neutron capture cross-section for $i^{\underline{th}}$ isotope, cm^2;
σ_i^f = fission cross-section for $i^{\underline{th}}$ isotope, cm^2;
ϕ = neutron flux, neutron cm^{-2} sec^{-1};
t = irradiation time, sec.

The average heat generation can be converted to an average heat flux for the rods by using the average neutron flux. The average neutron flux is proportional to the power level; thus, employing the proper conversion constants, the heat flux per megawatt is given by

$$(\overline{Q/A}) \sum_i (7660)(\sigma_i^f)(Mw)\, N_i(o) \exp - \left[(1.28 \times 10^{-6})(\sigma_i^f + \sigma_i^c)\, Mwd\right] \tag{12}$$

where

$(\overline{Q/A})$ = average heat flux, Btu hr^{-1} ft^{-2};
Mw = power level of reactor, megawatts;
σ_i^f = fission cross-section for $i^{\underline{th}}$ isotope, barns;
σ_i^c = capture cross-section for $i^{\underline{th}}$ isotope, barns;
d = irradiation time, days;
$N_i(o)$ = initial concentration of $i^{\underline{th}}$ isotope, moles/rod.

The average Al gamma heating in the target region[8] is assumed to be 0.65 watts per gram per megawatt. This can be converted to an average heat flux on a target rod by the relation

$$(\overline{Q/A}) = (1330)(Mw) \tag{13}$$

Combining Eqs. (12) and (13) for the total average heat flux gives

$$(\overline{Q/A}) = \sum_i \left\{7660\ \sigma_i^f\ N_i(o)\ \exp -\left[\left(1.78 \times 10^{-6}\right)\left(\sigma_i^f + \sigma_i^c\right) \text{Mwd}\right] + 1330\right\} (\text{Mw})\ . \tag{14}$$

The maximum-to-average nuclear peaking factors for the radial and axial direction are 1.06 and 1.29, respectively. In addition, a hot spot factor of 1.25 was chosen to cover all contingencies. The product of the above three factors with the combined average heat flux gives the peak or "hot spot" heat flux as

$$(Q/A) = \sum_i \left\{7660\ \sigma_i^f\ \text{Ni}(o)\ \exp -\left[\left(1.78 \times 10^{6}\right)\left(\sigma_i^f + \sigma_i^c\right) \text{Mwd}\right] + 1330\right\} (1.71)(\text{Mw}). \tag{15}$$

The heat removal for this case must satisfy the same restrictions as previously discussed. The only change will involve the assumptions made regarding the aluminum oxide formation on the outside surface of the containment tube. The target rods have not accumulated sufficient environmental exposure[5] to produce a thick Al_2O_3 film which negates assumptions 2 and 3 on page 6. Using the previous analysis with the above exceptions permits the maximum temperature in a rod to be written as

$$T = 622 + 224 \times 10^{-6}(Q/A) \tag{16}$$

where

T = maximum rod temperature, °F

(Q/A) = heat flux at the outside surface, Btu hr^{-1} ft^{-2}.

This equation was obtained by expressing the temperature changes as functions of the outside surface heat flux. Equation (4) was used with a 0.8-mil fabrication clearance to establish the temperature drop at the pellet-tube interface. A 900°F maximum temperature, a limitation previously discussed, is substituted into Eq. (16) and is solved for the heat flux as

$$Q/A = 1.24 \times 10^{6}\ . \tag{17}$$

This can be inserted into Eq. (15) along with the cross-sections for ^{239}Pu and ^{241}Pu to give the permissible power level as

$$Mw = \frac{1}{7.88\ N_1(o)\ e^{-0.00189\ Mwd} + 10.7\ N_2(o)\ e^{-0.00249\ Mwd} + 0.00184} \quad (18)$$

where

$N_1(o)$ = ^{239}Pu loading, moles/rod:
$N_2(o)$ = ^{241}Pu loading, moles/rod;
Mw = power level, megawatts;
d = irradiation time, days.

The material on hand[9] to fabricate the recommended target loading of 8.83 g of ^{242}Pu per rod will have ^{239}Pu and ^{241}Pu loadings of 0.0795 and 0.0892 g/rod, respectively. The solution of Eq. (18) for the above concentrations per rod gave a permissible nominal reactor power level of 120 Mw at the beginning of a target irradiation. This allowable power level permits substitution of unirradiated target rods that are fabricated with the aforementioned ^{239}Pu and ^{241}Pu rod concentrations for irradiated target rods without altering the normal reactor operating power level.

The final calculation made for the target rod design was the burnout heat flux. A pressure of 200 psia and a water temperature of 140°F gave a minimum burnout heat flux of 3.8×10^6 Btu hr^{-1} ft^{-2}, utilizing Gambills' burnout heat flux equation.[4] The above burnout heat flux gives a factor of 3 or greater for the burnout margin at any time during the target rod irradiation cycle. This is a conservative calculation because the nominal operating pressure is 600 psia and the reactor scram point is set at 375 psi.

IRRADIATION OF TARGET PROTOTYPES

Four HFIR target-prototype irradiation rods[10] were inserted in the ETR on October 28, 1963, and irradiated with an average heat flux of about 0.6×10^6 Btu hr^{-1} ft^{-2}. The first of the rods was removed on April 13, 1964, after an estimated peak unperturbed exposure of 1.7×10^{21} neutrons/cm^2. The remaining three rods are still being irradiated as planned, to

a level of integrated, peak, unperturbed exposure of 3.2×10^{21} neutrons/cm^2. However, to evaluate a prototype exposed to average conditions which closely approach the predicted operating hot-spot conditions in HFIR, plans are under way to irradiate one prototype in a peak unperturbed thermal flux of 3.75×10^{14} neutrons/cm^{-2} sec^{-1}. In this neutron flux, the prototype will be subject to an average heat flux of 10^6 Btu hr^{-1} ft^{-2}.

With the exception of some detailed metallography, the examination of the first target prototype is nearly complete. The tubing-to-hex-can spacing and length of the capsule were unchanged. The capsule-to-hex-can attachments were sound. All surfaces of the aluminum were covered with a thin layer of off-white oxide. Gamma-ray scanning indicated almost uniform flux distribution, with a slight peak about 4 1/2 in. from the top of the pellet column. Cobalt-activation analysis of the central aluminum fin indicated an integrated flux exposure of 1.27×10^{21} nvt. Subsequent burnup analyses from the peak pellet, which was about 10% above the average, indicated a heavy-element burnup of 44 at. % (31 at. % fissioning or 1.1×10^{21} fissions/cc in the fuel composite). The peak-to-average ratio and the actual fissioning are in remarkable agreement with the preirradiation predictions and thus tend to substantiate all the operating conditions intended to be comparable with the actual HFIR targets.

Fission-gas samples were taken from three locations on the prototype, from each of the void spaces provided at the ends of the target and one by drilling into a centrally located pellet. The amount of gas removed from these regions indicated that there was nearly a complete separation of the voids, one from another, and that up to this level of irradiation most of the gas was retained within the pellets. Based on the ^{85}Kr recovered from both of the end plenums, less than 2% of the fission gas had been released to the plenums.

The rod was sectioned through the fuel material which revealed a tightly packed fuel sample with no apparent gap between the various tubes. There was no evidence of melting or void formation in any of the sections.

REFERENCES

1. R. D. Cheverton, HFIR Preliminary Physics Report, ORNL-3006 (October 4, 1960).
2. H. C. Claiborne and M. P. Lietzke, Californium Production in the High Flux Isotope Reactor, ORNL-CF-59-8-125 (August 31, 1959).
3. James Replogle, Modric, A One Dimension Neutron Diffusion Code for the IBM 7090, K-1497, UCND-ORGDP (1962).
4. W. R. Gambill and R. D. Bundy, HFIR Heat-Transfer Studies of Turbulent Water Flow in Thin Rectangular Channels, ORNL-3079 (June 5, 1961).
5. J. C. Griess, H. C. Savage, and J. L. English, Effect of Heat Flux on the Corrosion of Aluminum by Water, Part IV. Tests Relative to the Advanced Test Reactor and Correlation with Previous Results, ORNL-3541 (February 1964).
6. H. Fenech and W. M. Rohsenow, Prediction of Thermal Conductance of Metallic Surfaces in Contact, Journal of Heat Transfer, p. 15 (February 1963).
7. H. Etherington, Nuclear Engineering Handbook, pp. 10-25 and 10-50.
8. D. R. Vondy, Gamma Ray and Neutron Heat Generation in the HFIR, ORNL-CF-63-2-52 (February 21, 1963).
9. J. P. Nichols, Gamma and Neutron Radiation from As-Fabricated TRU-HFIR Target Rods, ORNL-CF-63-10-64 (October 28, 1963).
10. W. D. Burch, et al., Transuranium Quart. Progr. Rept. Aug. 31, 1964, ORNL-3739.

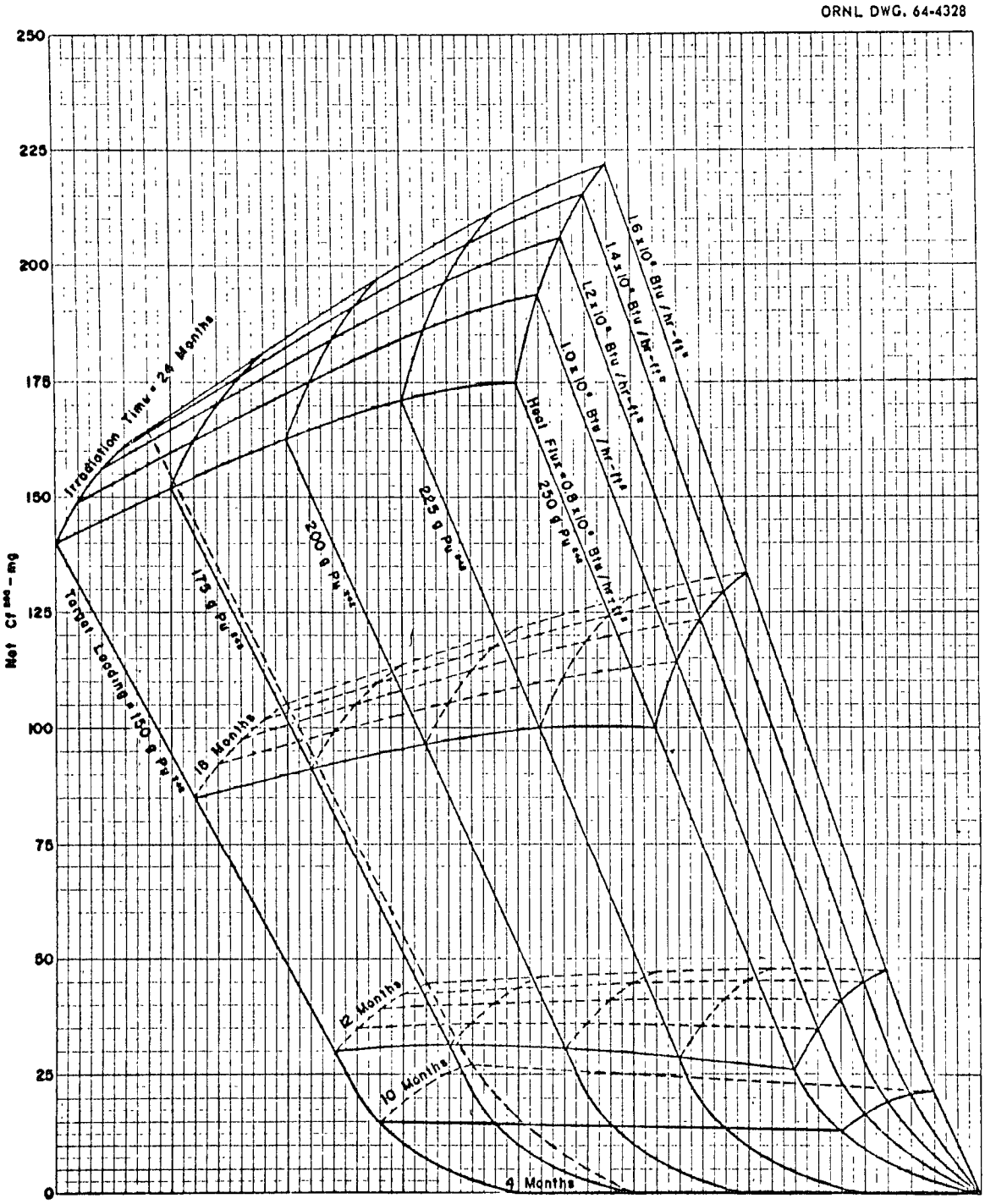

Fig. 1. Parametric Study of ^{252}Cf Production in HFIR.

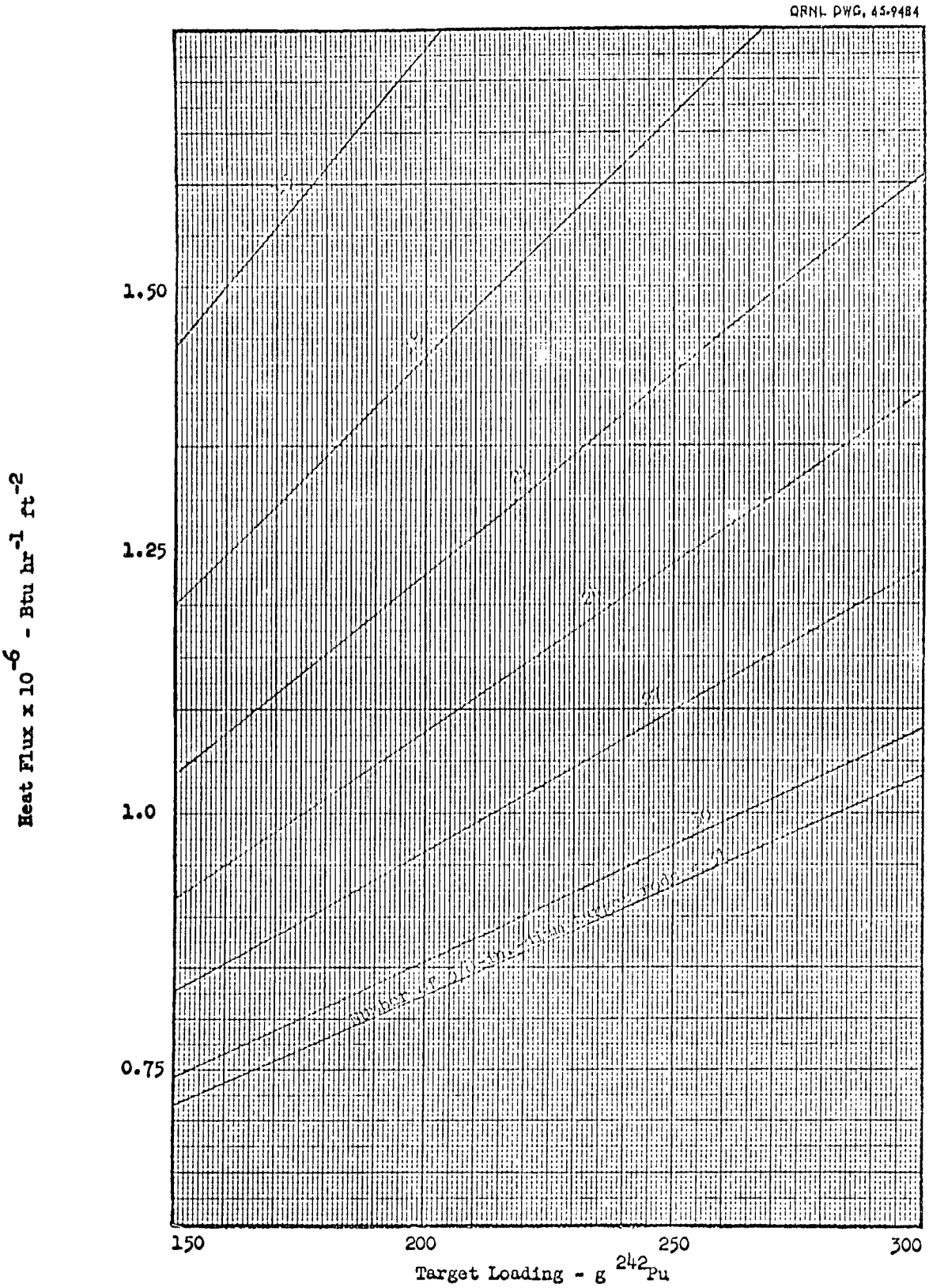

Fig. 2. HFIR Target Heat Removal.

ORNL-DWG 65-1383

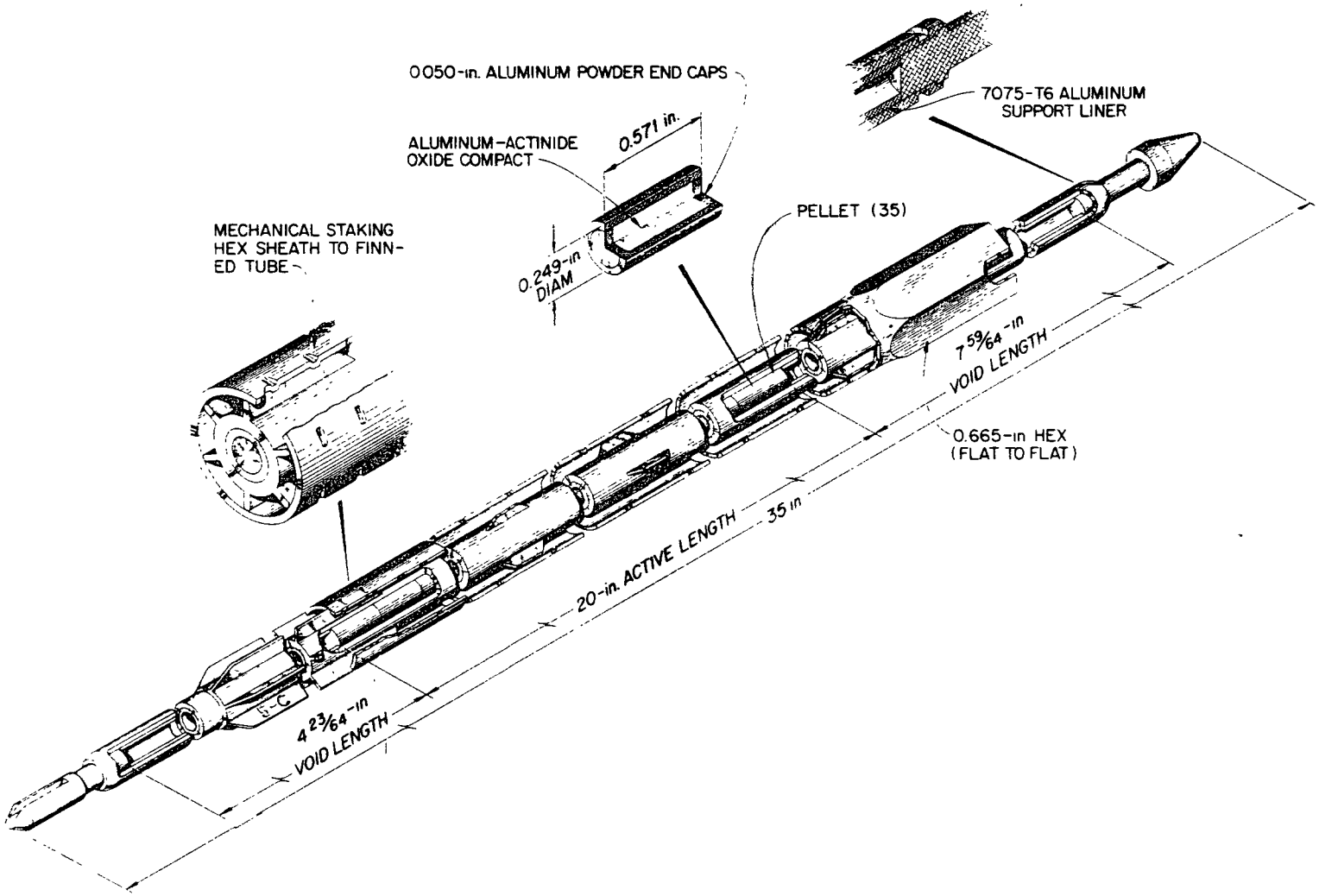

Fig. 3. HFIR Target Rod Design.

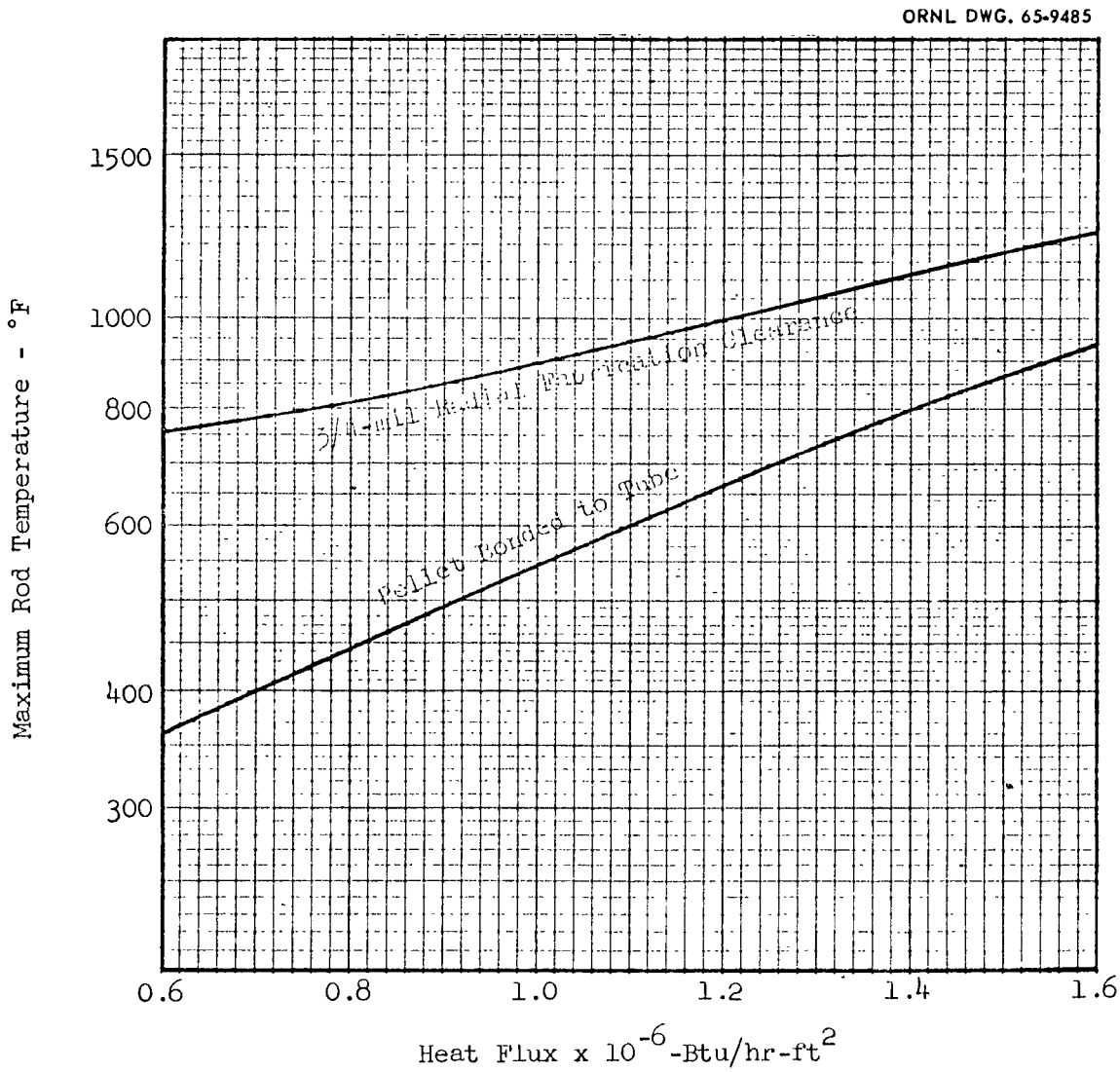

Fig. 4. Maximum HFIR Target Rod Temperatures.

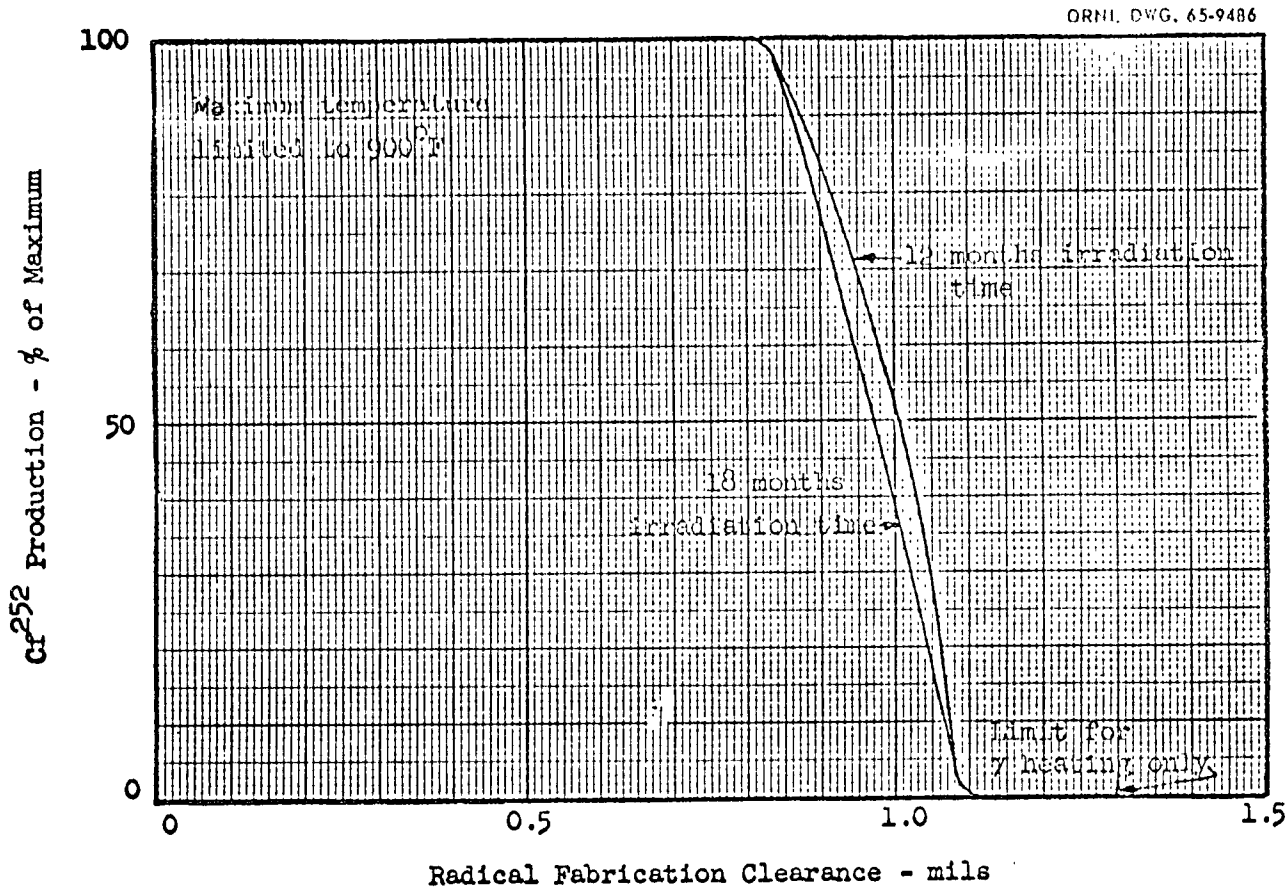

Fig. 5. Effect of Clearance Between Pellet and Containment Tube on ^{252}Cf Production.

Internal Distribution

1. G. M. Adamson, Jr.
2. S. E. Beall
3. R. J. Beaver
4. E. S. Bettis
5. F. T. Binford
6. A. L. Boch
7. E. G. Bohlmann
8. R. B. Briggs
9. F. R. Bruce
10. W. D. Burch
11. T. J. Burnett
12. C. D. Cagle
13. T. G. Chapman
14. A. Chetham-Strode
15. R. D. Cheverton
16. H. C. Claiborne
17. W. G. Cobb
18. T. E. Cole
19. W. B. Cottrell
20. J. A. Cox
21. E. N. Cramer
22. F. L. Culler
23. J. E. Cunningham
24. B. C. Duggins
25. E. P. Epler
26. W. K. Ergen
27. D. E. Ferguson
28. A. P. Fraas
29. W. R. Gambill
30. J. C. Griess
31. L. A. Haack
32. P. N. Haubenreich
33. J. W. Hill, Jr.
34. R. M. Hill, Jr.
35. J. E. Jones, Jr.
36. P. R. Kasten
37. W. C. Koehler
38. J. A. Lane
39. M. I. Lundin
40. R. N. Lyon
41. H. G. MacPherson
42. R. V. McCord
43. H. C. McCurdy
44. H. A. McLain
45. J. R. McWherter
46. A. J. Miller
47. L. C. Oakes
48. A. R. Olsen
49. A. M. Perry
50. J. T. Roberts
51. M. W. Rosenthal
52. H. W. Savage
53. A. W. Savolainen
54. R. E. Schappel
55. D. Scott, Jr.
56. T. M. Sims
57. M. J. Skinner
58. I. Spiewak
59. P. N. Stevens
60. R. S. Stone
61. D. B. Trauger
62. A. M. Weinberg
63. J. H. Westsik
64. M. K. Wilkinson
65. G. D. Whitman

66-67. Central Research Library (CRL)
68-69. Y-12 Document Reference Section (DRS)
70-72. Laboratory Records Department (LRD)
73. Laboratory Records Department - Record Copy (LRD-RC)

External Distribution

74. T. R. Jones, Division of Research, AEC, Washington
75-89. Division of Technical Information Extension (DTIE)
90. Research and Development Division, AEC, ORO
91-93. Reactor Division, AEC, ORO